

# Direct Numerical Simulation of a 2D heat exchanger based on circular cylinders

---



**Supervisor:** Prof Sylvain Laizet  
**Department:** Department of Aeronautics  
**Course:** AERO70008  
**Author:** Jason Zhao  
**Date:** 30/06/2025

Department of Aeronautics  
South Kensington Campus  
Imperial College London  
London SW7 2AZ  
U.K.

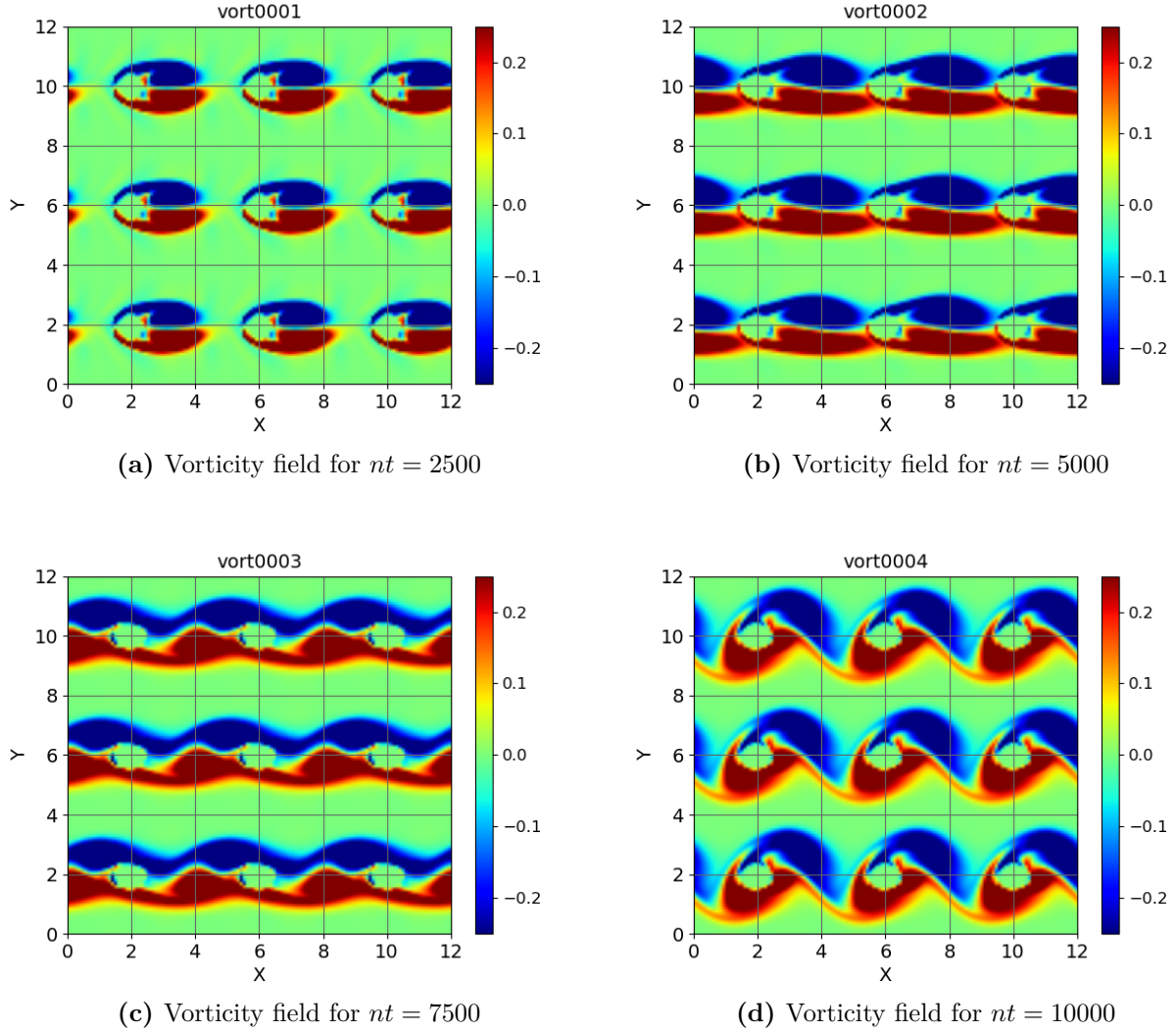
# Contents

Table of Contents	i
1 Baseline Simulation with Second-Order Adams-Bashforth	1
2 Stability Analysis with Increased CFL	2
3 Implementing a Third-Order Runge-Kutta Scheme	3
4 Implementing Fourth-Order Centered Differences	5
5 Long-Term Flow Behavior Analysis	8
6 Reverse Flow Direction Simulation	9
7 Simulation of a Single Cylinder with Inflow/Outflow Boundary Conditions	10

# 1 Baseline Simulation with Second-Order Adams-Bashforth

The results demonstrate numerical stability under given perturbation, and shows typical pattern under given Reynolds number. The vortices formed behind the cylinder with maximum range around 0.22. The upper vortices are clockwise and lowers are anticlockwise.

From  $nt = 7500$  onward, alternative periodic vortex sheddings develop downstream the cylinders, and they influence each other and formed typical Karman vortex street [1]. Hence, the simulation demonstrates expected flow features for a subcritical Reynolds number regime.

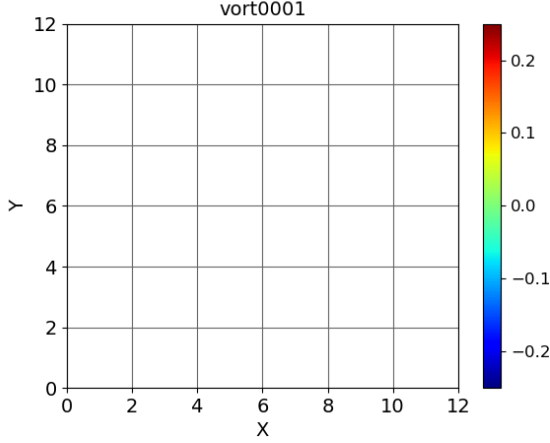


**Figure 1.** Time evolution of the vorticity field for different time steps ( $nt = 2500, 5000, 7500, 10000$ ) using the second-order Adams-Bashforth scheme with  $Re = 200$  and  $CFL = 0.25$ .

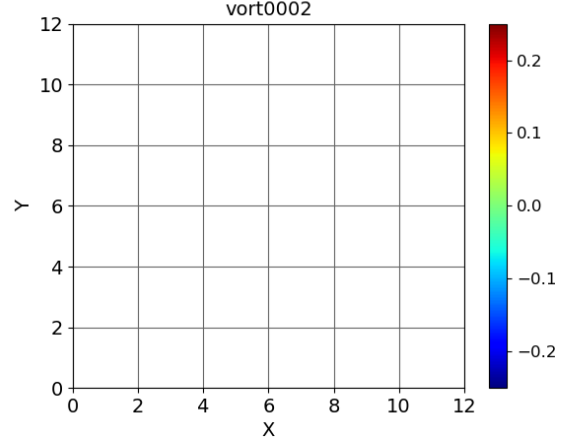
## 2 Stability Analysis with Increased CFL

There is no meaningful result generated. The numerical values grew unbounded and the scheme becomes numerically unstable. Adams-Bashforth is an explicit scheme, thus sensitive to time step, which is determined by CFL condition (1). Large time step causing oscillation and eventually grow unbounded.  $CFL = 0.75$  is above the threshold value and caused unstable

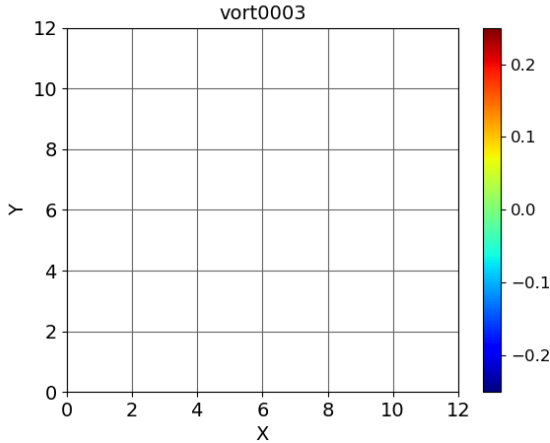
$$CFL = \frac{u \Delta t}{\Delta x} \leq (\text{Threshold Value}). \quad (1)$$



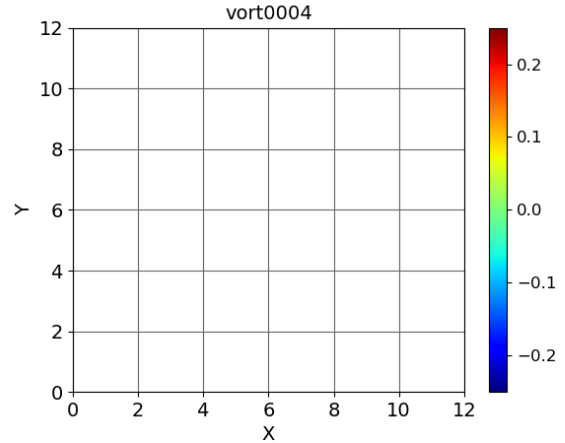
(a) Vorticity field for  $nt = 2500$



(b) Vorticity field for  $nt = 5000$



(c) Vorticity field for  $nt = 7500$



(d) Vorticity field for  $nt = 10000$

**Figure 2.** Time evolution of the vorticity field for different time steps ( $nt = 2500, 5000, 7500, 10000$ ) using the second-order Adams-Bashforth scheme with  $Re = 200$  and  $CFL = 0.75$ . No meaningful results generated.

### 3 Implementing a Third-Order Runge-Kutta Scheme

The third order Runge-Kutta scheme remains stable and confirming robust robustness at  $CFL = 0.75$ . Compared with second-order Adams-Bashforth, the higher-order Runge-Kutta scheme captures finer details, and has a larger stability region. Compared to Second-Order Adams-Bashforth scheme, Runge-Kutta has more accuracy at high frequency and phase error, allowing it remains stable at a larger time step. Meanwhile, larger time step reduces the computational cost. Figure 3a and Figure 1c are the same time second simulation and shows the same pattern vortex sheddings.

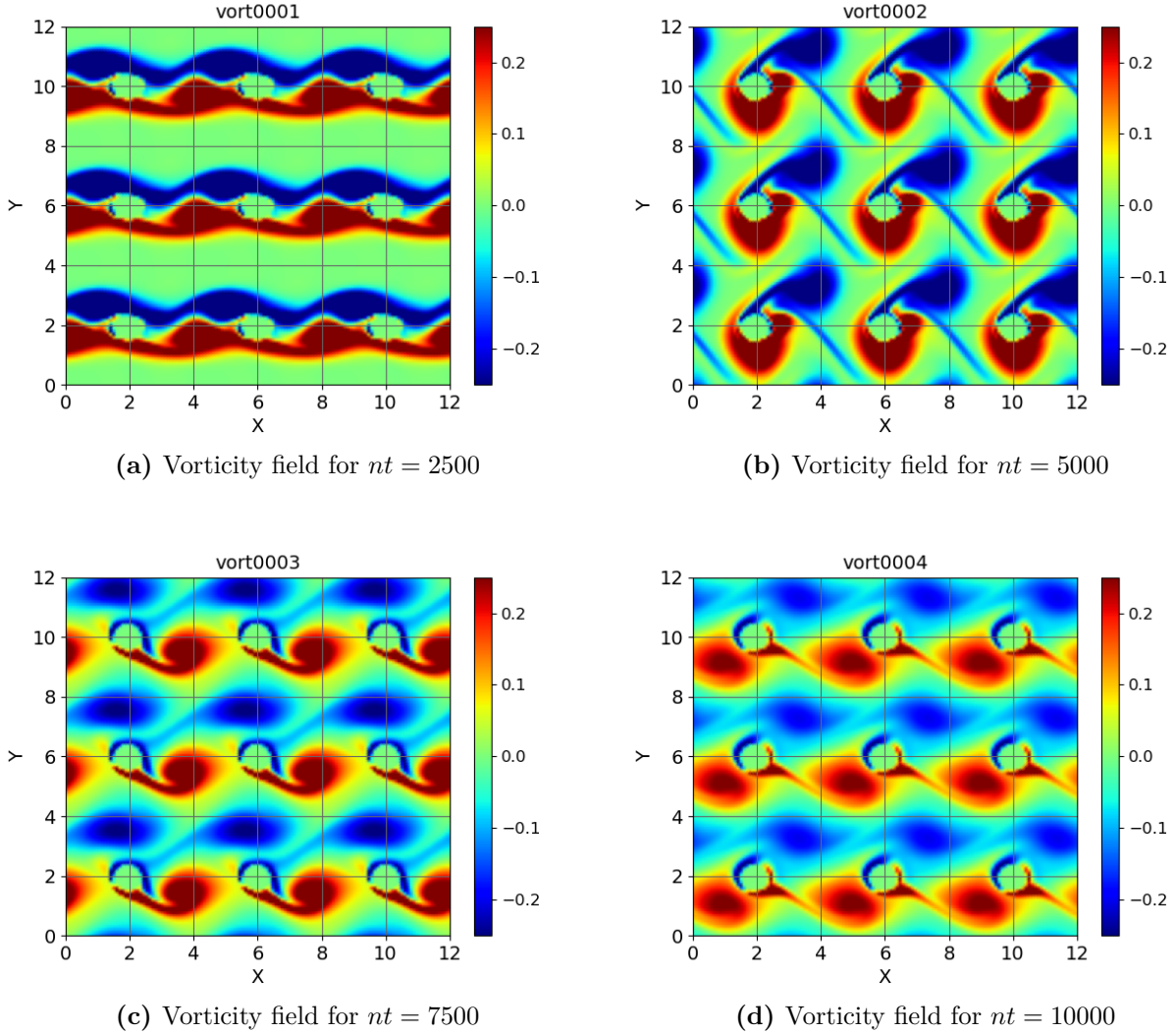


**Figure 3.** Time evolution of the vorticity field for different time steps ( $nt = 2500, 5000, 7500, 10000$ ) using the third-order Runge-kutta scheme with  $Re = 200$  and  $CFL = 0.75$ .

• Subroutine **rkutta()**:

```

1  subroutine rkutta(rho,rou,rov,roe,fro,gro,fru,gru,frv,grv,&
2     fre,gre,nx,ny,ns,dlt,coef,k)
3  !
4  ! #####
5
6  implicit none
7  !
8  real(8),dimension(nx,ny) :: rho,rou,rov,roe,fro,gro,fru,gru,frv
9  real(8),dimension(nx,ny) :: grv,fre,gre
10 real(8),dimension(2,ns) :: coef

```

```

11  real(8) :: dlt
12  integer :: i,j,nx,ny,ns,k
13  !
14  !coefficient for RK sub-time steps
15  coef(1,1)=8./15.
16  coef(1,2)=5./12.
17  coef(1,3)=3./4.
18  coef(2,1)=0.
19  coef(2,2)=-17./60.
20  coef(2,3)=-5./12.
21
22  do j=1,ny
23      do i=1,nx
24  !!
25          rho(i,j)=rho(i,j)+dlt*(coef(1,k)*fro(i,j)+coef(2,k)*gro(i,j))
26          gro(i,j)=fro(i,j)!g is k-1
27          rou(i,j)=rou(i,j)+dlt*(coef(1,k)*fru(i,j)+coef(2,k)*gru(i,j))
28          gru(i,j)=fru(i,j)
29          rov(i,j)=rov(i,j)+dlt*(coef(1,k)*frv(i,j)+coef(2,k)*grv(i,j))
30          grv(i,j)=frv(i,j)
31          roe(i,j)=roe(i,j)+dlt*(coef(1,k)*fre(i,j)+coef(2,k)*gre(i,j))
32          gre(i,j)=fre(i,j)
33
34      enddo
35  enddo
36
37  return
38 end subroutine rkutta

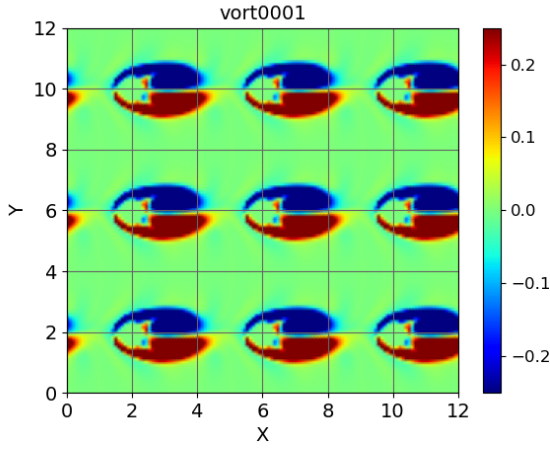
```

## 4 Implementing Fourth-Order Centered Differences

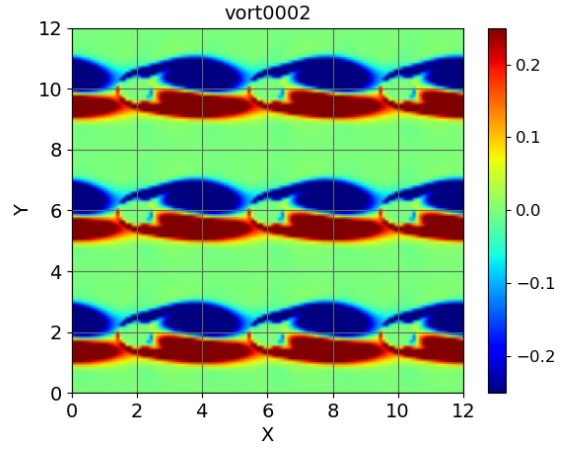
The centered fourth-order schemes are computed from Taylor's expansion as equations (2) and (3). Compared to task 1, a longer computational time is seen as more points involved in computations. It is expected that centered fourth-order schemes should have less dissipation and dispersion error, capturing finer details such as turbulence, small vortices, and shear layer [2]. However, no significant difference is seen. This might be due to the large grid size which also causes the error, or due to time step  $\Delta t$  too small, making the advantage of higher order scheme difficult to be seen.

$$\left. \frac{d\phi}{dx} \right|_i \approx \frac{-\phi_{i+2} + 8\phi_{i+1} - 8\phi_{i-1} + \phi_{i-2}}{12\Delta x} \quad (2)$$

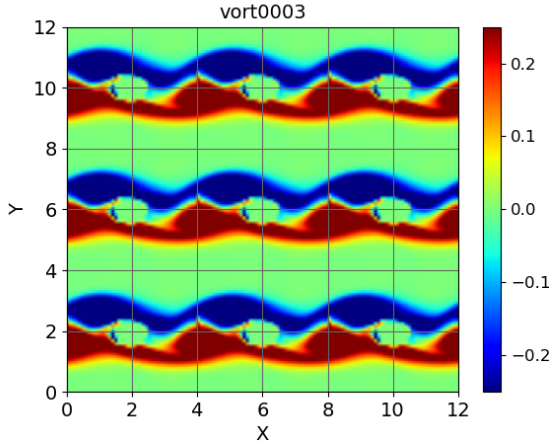
$$\left. \frac{d^2\phi}{dx^2} \right|_i \approx \frac{-\phi_{i+2} + 16\phi_{i+1} - 30\phi_i + 16\phi_{i-1} - \phi_{i-2}}{12(\Delta x)^2} \quad (3)$$



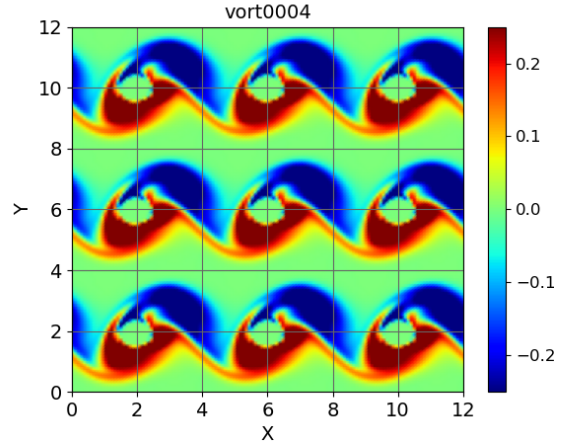
(a) Vorticity field for  $nt = 2500$



(b) Vorticity field for  $nt = 5000$



(c) Vorticity field for  $nt = 7500$



(d) Vorticity field for  $nt = 10000$

**Figure 4.** Time evolution of the vorticity field for different time steps ( $nt = 2500, 5000, 7500, 10000$ ) using the second-order Adams-Bashforth scheme with  $Re = 200$  and  $CFL = 0.25$ .

- Subroutine **derix4()**, **deriy4()**, **derxx4()**, and **deryy4()**:

```
1 subroutine derix4(phi,nx,ny,dfi,xlx)
2 !
3 !Fourth-order first derivative in the x direction
```



```

4  ! #####
5
6  implicit none
7
8  real(8),dimension(nx,ny) :: phi,dfi
9  real(8) :: dlx,plx,udx
10 integer :: i,j,nx,ny
11
12
13  dlx=plx/nx
14  udx=1./(12.*dlx)    !updated multiplier
15  do j=1,ny
16      dfi(1,j)=udx*(-phi(3,j)+8.*phi(2,j)-8.*phi(nx,j)+phi(nx-1,j))    !Boundary
17          Condition: i=1
18      dfi(2,j)=udx*(-phi(4,j)+8.*phi(3,j)-8.*phi(1,j)+phi(nx,j))    !Boundary Condition:
19          i=2
20      do i=3,nx-2
21          dfi(i,j)=udx*(-phi(i+2,j)+8.*phi(i+1,j)-8.*phi(i-1,j)+phi(i-2,j))    !i=3 to nx-2
22      enddo
23      dfi(nx-1,j)=udx*(-phi(1,j)+8.*phi(nx,j)-8.*phi(nx-2,j)+phi(nx-3,j))    !Boundary
24          Condition: i=nx-1
25      dfi(nx,j)=udx*(-phi(2,j)+8.*phi(1,j)-8.*phi(nx-1,j)+phi(nx-2,j))    !Boundary
26          Condition: i=nx
27  enddo
28
29  return
30 end subroutine derix4
31 ! #####
32 ! #####
33 !
34 subroutine deriy4(phi,nx,ny,dfi,ply)
35 !
36 !Fourth-order first derivative in the y direction
37 ! #####
38
39 implicit none
40
41 real(8),dimension(nx,ny) :: phi,dfi
42 real(8) :: dly,ply,udy
43 integer :: i,j,nx,ny
44
45 dly=ply/ny !dly:grid size; ply: total length
46 udy=1./(12.*dly)    !updated multiplier
47 do j=3,ny-2
48     do i=1,nx
49         dfi(i,j)=udy*(-phi(i,j+2)+8.*phi(i,j+1)-8.*phi(i,j-1)+phi(i,j-2))    !j=3 to ny-2
50     enddo
51 enddo
52 do i=1,nx !Boundary Condition
53     dfi(i,1)=udy*(-phi(i,3)+8.*phi(i,2)-8.*phi(i,ny)+phi(i,ny-1))    !Boundary
54         Condition: j=1
55     dfi(i,2)=udy*(-phi(i,4)+8.*phi(i,3)-8.*phi(i,1)+phi(i,ny))    !Boundary Condition:
56         j=2
57     dfi(i,ny-1)=udy*(-phi(i,1)+8.*phi(i,ny)-8.*phi(i,ny-2)+phi(i,ny-3))    !Boundary
58         Condition: j=ny-1
59     dfi(i,ny)=udy*(-phi(i,2)+8.*phi(i,1)-8.*phi(i,ny-1)+phi(i,ny-2))    !Boundary
60         Condition: j=ny
61 enddo
62
63 return
64 end subroutine deriy4
65 ! #####

```



```

61
62 !#####
63 !
64 subroutine derxx4(phi,nx,ny,dfi,plx)
65 !
66 !Fourth-order second derivative in y direction
67 !#####
68
69 implicit none
70
71 real(8),dimension(nx,ny) :: phi,dfi
72 real(8) :: dlx,plx,udx
73 integer :: i,j,nx,ny
74
75 dlx=plx/nx
76 udx=1./(12.*dlx*dlx) !updated multiplier
77 do j=1,ny
78   dfi(1,j)=udx*(-phi(3,j)+16.*phi(2,j)-30.*phi(1,j)+16.*phi(nx,j)-phi(nx-1,j))
79   !Boundary Condition: i=1
80   dfi(2,j)=udx*(-phi(4,j)+16.*phi(3,j)-30.*phi(2,j)+16.*phi(1,j)-phi(nx,j))
81   !Boundary Condition: i=2
82   do i=3,nx-2
83     dfi(i,j)=udx*(-phi(i+2,j)+16.*phi(i+1,j)-30.*phi(i,j)+16.*phi(i-1,j)-phi(i-2,j))
84     !i=3 to nx-2
85   enddo
86   dfi(nx-1,j)=udx*(-phi(1,j)+16.*phi(nx,j)-30.*phi(nx-1,j)+16.*phi(nx-2,j)-phi(nx-3,j))
87   !Boundary Condition: i=nx-1
88   dfi(nx,j)=udx*(-phi(2,j)+16.*phi(1,j)-30.*phi(nx,j)+16.*phi(nx-1,j)-phi(nx-2,j))
89   !Boundary Condition: i=nx
90 enddo
91
92 return
93 end subroutine derxx4
94 !#####
95 !#####
96 !
97 subroutine deryy4(phi,nx,ny,dfi,ply)
98 !
99 !Fourth-order second derivative in the y direction
100 !#####
101
102 implicit none
103
104 real(8),dimension(nx,ny) :: phi,dfi
105 real(8) :: dly,ply,udy
106 integer :: i,j,nx,ny
107
108 dly=ply/ny
109 udy=1./(12.*dly*dly) !updated multiplier
110 do j=3,ny-2
111   do i=1,nx
112     dfi(i,j)=udy*(-phi(i,j+2)+16.*phi(i,j+1)-30.*phi(i,j)+16.*phi(i,j-1)-phi(i,j-2))
113     !j=3 to ny-2
114   enddo
115 enddo
116 do i=1,nx
117   dfi(i,1)=udy*(-phi(i,3)+16.*phi(i,2)-30.*phi(i,1)+16.*phi(i,ny)-phi(i,ny-1))
118   !Boundary Condition: j=1
119   dfi(i,2)=udy*(-phi(i,4)+16.*phi(i,3)-30.*phi(i,2)+16.*phi(i,1)-phi(i,ny)) !Boundary
120   Condition: j=2
121   dfi(i,ny-1)=udy*(-phi(i,1)+16.*phi(i,ny)-30.*phi(i,ny-1)+16.*phi(i,ny-2)-phi(i,ny-3))
122   !Boundary Condition: j=ny-1
123   dfi(i,ny)=udy*(-phi(i,2)+16.*phi(i,1)-30.*phi(i,ny)+16.*phi(i,ny-1)-phi(i,ny-2))

```

```

117         !Boundary Condition: j=ny
118     enddo
119
120     return
121 end subroutine deryy4
122 !#####

```

## 5 Long-Term Flow Behavior Analysis

When the simulation continues, the vortex shedding begin to vanish, and the flow becomes uniformed. The numerical value of the simulation gradually dissipates, and the outline of the vortices becomes blurry. This is due to the dissipation of the second-order Adams-Bashforth scheme and finite difference, and the boundary condition which smooth out the small-scale vortices.

## 6 Reverse Flow Direction Simulation

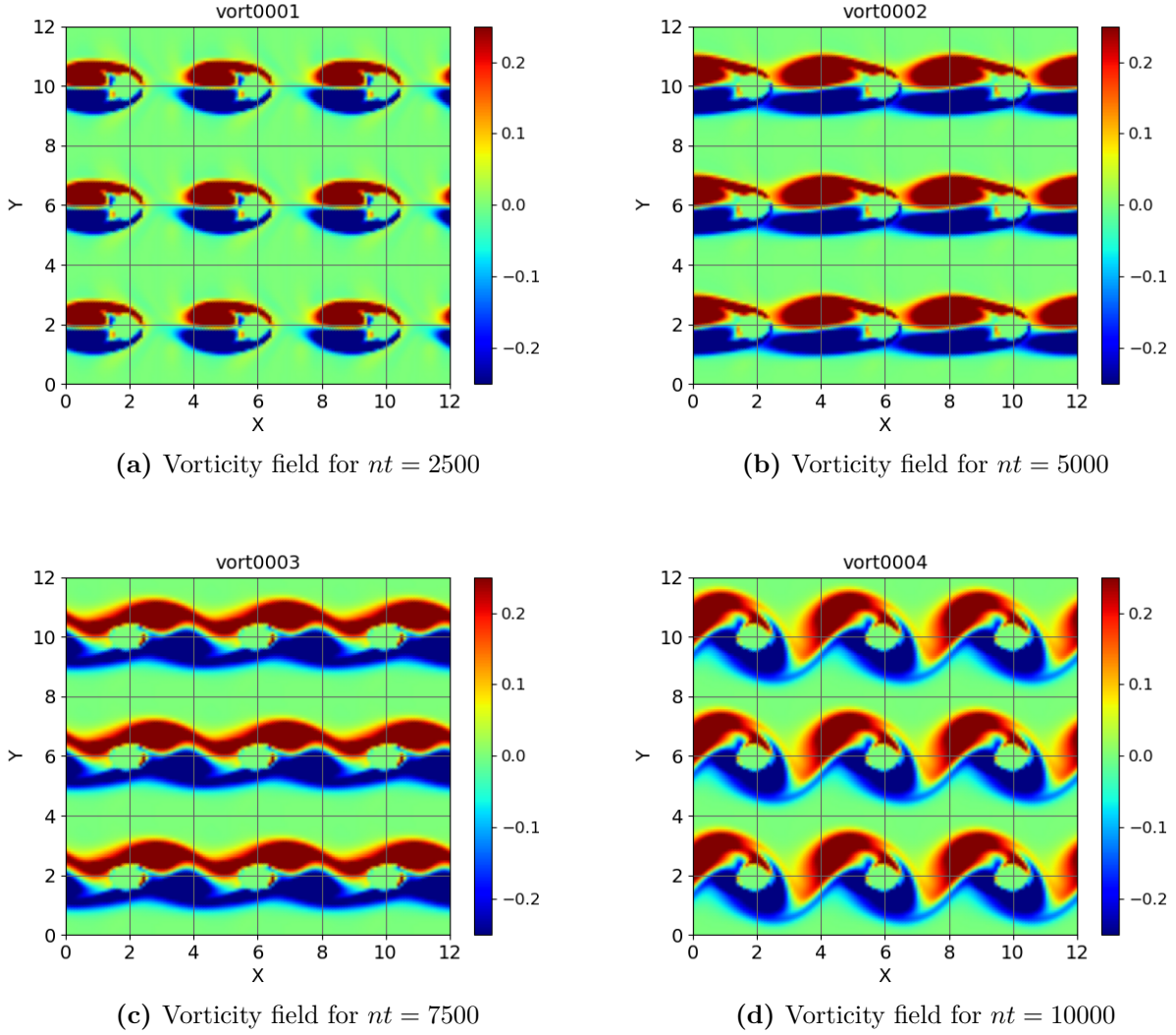


**Figure 5.** Time evolution of the vorticity field for different time steps ( $nt = 2500, 5000, 7500, 10000$ ) using the second-order Adams-Bashforth scheme with  $Re = 200$  and  $CFL = 0.25$ , with flow coming from right to left.

- In the subroutine `initl`, change `uuu` to the negative direction.

```
1  uuu(i,j)=-uu0    !negative
```

- Additional: change the index of y-direction turbulence to  $nx + 1 - i$  to get a more accurate mirrored pattern the original case.

```
1  vvv(i,j)=0.01*(sin(4.*pi*(nx+1-i)*dlx/xlx)&
2    +sin(7.*pi*(nx+1-i)*dlx/xlx))*&
3    exp(-(j*dly-yly/2.))**2)
```

## 7 Simulation of a Single Cylinder with Inflow/Outflow Boundary Conditions

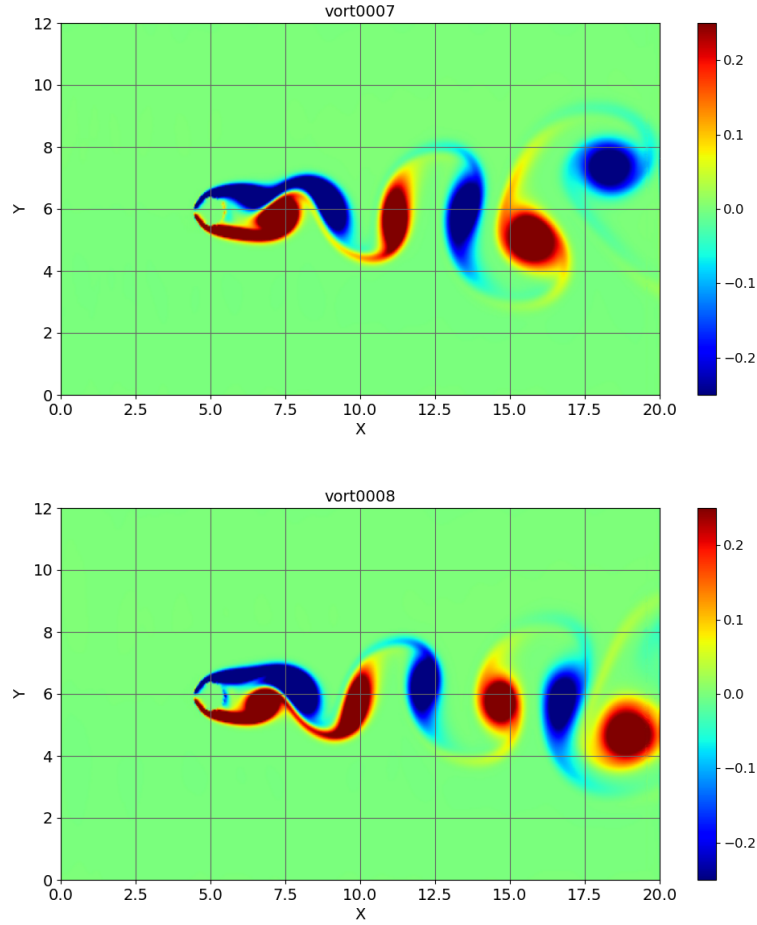


**Figure 6.** *Instantaneous visualisations of the flow around a single cylinder with inflow/outflow boundary conditions in the streamwise direction.*

### 1. New subroutine **boundary()**:

```

1  subroutine boundary(uuu,vvv,rho,eee,tmp,rou,rov,roe,nx,ny,&
2  xlx,yly,xmu,xba,gma,dlx,dlt,uu0)
3
4      implicit none
5
6      real(8),dimension(nx,ny) :: uuu,vvv,rho,eee,tmp,rou,rov,roe
7      real(8) :: xlx,yly,xmu,xba,gma,roi,cci,d,tpi,chv,uu0
8      real(8) :: pi,dlx,dly,dlt,ct6
9      integer :: nx,ny,j
10
11     call param(xlx,yly,xmu,xba,gma,roi,cci,d,tpi,chv,uu0)
12
13     ct6=(gma-1.)/gma
14     pi=acos(-1.)
15
16     !#####Inlet Condition#####
17     do j=1,ny
18         uuu(1,j)=uu0
19         vvv(1,j)=0.01*(sin(4.*pi*(1)*dlx/xxl)&

```

```

20         +sin(7.*pi*(1)*dlx/xlx))*&
21         exp(-(j*dly-yly/2.))**2)
22     tmp(1,j)=tpi
23     eee(1,j)=chv*tmp(1,j)+0.5*(uuu(1,j)*uuu(1,j)+vvv(1,j)*vvv(1,j))
24     rho(1,j)=roi
25     rou(1,j)=rho(1,j)*uuu(1,j)
26     rov(1,j)=rho(1,j)*vvv(1,j)
27     roe(1,j)=rho(1,j)*eee(1,j)
28 enddo
29
30 !#####Outlet Condition#####
31 do j=1,ny
32     rho(nx,j)=rho(nx,j)-uu0*dlt/dlx*(rho(nx,j)-rho(nx-1,j))
33     rou(nx,j)=rou(nx,j)-uu0*dlt/dlx*(rou(nx,j)-rou(nx-1,j))
34     rov(nx,j)=rov(nx,j)-uu0*dlt/dlx*(rov(nx,j)-rov(nx-1,j))
35     roe(nx,j)=roe(nx,j)-uu0*dlt/dlx*(roe(nx,j)-roe(nx-1,j))
36
37 enddo
38
39 return
40 end subroutine boundary

```

## 2. Modified subroutine **derix()**:

```

1  subroutine derix(phi,nx,ny,dfi,plx)
2  !
3  !First derivative in the x direction
4  !#####
5
6  implicit none
7
8  real(8),dimension(nx,ny) :: phi,dfi
9  real(8) :: plx,plx,udx
10 integer :: i,j,nx,ny
11
12 plx=plx/nx
13 udx=1./(plx+plx)
14 do j=1,ny
15     !Inlet Condition, First order forward difference scheme
16     dfi(1,j)=(1./plx)*(phi(2,j)-phi(1,j))
17     do i=2,nx-1
18         dfi(i,j)=udx*(phi(i+1,j)-phi(i-1,j))
19     enddo
20     !Outlet Condition, First order backward difference scheme
21     dfi(nx,j)=(1./plx)*(phi(nx,j)-phi(nx-1,j))
22 enddo
23
24 return
25 end subroutine derix

```

## 3. Modified subroutine **derxx()**:

```

1  subroutine derxx(phi,nx,ny,dfi,plx)
2  !
3  !Second derivative in x direction
4  !#####
5
6  implicit none
7
8  real(8),dimension(nx,ny) :: phi,dfi
9  real(8) :: plx,plx,udx
10 integer :: i,j,nx,ny
11

```

```

12  dlx=xlx/nx
13  udx=1./(dlx*dlx)
14  do j=1,ny
15      !Inlet Boundary Condition, Second-order one-sided difference scheme
16      dfi(1,j)=udx*((phi(1,j)+phi(1,j))-5.*phi(2,j)+4.*phi(3,j)-phi(4,j))
17      do i=2,nx-1
18          dfi(i,j)=udx*(phi(i+1,j)-(phi(i,j)+phi(i,j))&
19              +phi(i-1,j))
20      enddo
21      !Outlet Boundary Condition, Second-order one-sided difference scheme
22      dfi(nx,j)=udx*((phi(nx,j)+phi(nx,j))-5.*phi(nx-1,j)+4.*phi(nx-2,j)-phi(nx-3,j))
23  enddo
24
25  return
26  end subroutine derxx

```

4. Additional. Implementing subroutine **boundary** in the time loop:

```

1      call adams(rho,rou,rov,roe,fro,gro,fru,gru,frv,grv,&
2          fre,gre,nx,ny,dlt)
3
4      !Imposing Boundary Condition
5      call boundary(uuu,vvv,rho,eee,tmp,rou,rov,roe,nx,ny,&
6          xlx,ylx,xmu,xba,gma,dlx,dlt,uu0)
7
8      call state(uuu,vvv,rho,pre,tmp,rou,rov,roe,nx,ny,gma)

```

5. Additional. Layout amendments in the **2D\_compressible.f90** file:

```

1      !nx->513, ny->257, nf->1
2      integer,parameter :: nx=513,ny=257,nt=15000,ns=3,nf=1,mx=nf*nx,my=nf*ny

```

```

1      !#####CIRCULAR CYLINDER DEFINITION#####
2      do j=1,ny
3          do i=1,nx
4              !Centre of cylinder located at (5d,6d)
5              if (((i*dlx-5.d0)**2+(j*dly-6.d0)**2).lt.radius**2) then
6                  eps(i,j)=1.
7              else
8                  eps(i,j)=0.
9              end if
10          enddo
11      enddo

```

```

1      xlx=20.*d      !DOMAIN SIZE X DIRECTION
2      yly=12.*d      !DOMAIN SIZE Y DIRECTION

```

6. Additional. Layout amendments in the **plot\_py** file:

```

1      #nx->513, ny->257, lx->20.0, ly->12.0
2      nx=513
3      ny=257
4      lx=20.0
5      ly=12.0
6
7      #12->lx
8      X=np.linspace(0,lx,num=nx)

```

```
1 #plot
2 fig,ax = plt.subplots(figsize=(12,6))
3 plt.figure((i+1),figsize=(20,12), edgecolor='none')
```



## References

- [1] Cooper JE. AEROELASTIC RESPONSE. In: Braun S, editor. Encyclopedia of Vibration. Oxford: Elsevier; 2001. p. 87-97. Available from: <https://www.sciencedirect.com/science/article/pii/B0122270851001259>.
- [2] Wang ZJ, Fidkowski K, Abgrall R, Bassi F, Caraeni D, Cary A, et al. High-Order CFD Methods: Current Status and Perspective. International Journal for Numerical Methods in Fluids. 2013;72(8):811-45. Available from: [https://www.researchgate.net/publication/236950745\\_High-Order\\_CFD\\_Methods\\_Current\\_Status\\_and\\_Perspective](https://www.researchgate.net/publication/236950745_High-Order_CFD_Methods_Current_Status_and_Perspective).